

# EchoAgent: Towards Reliable Echocardiography Interpretation with “Eyes”, “Hands” and “Minds”

Qin Wang<sup>1</sup>, Zhiqing He<sup>1</sup>, Yu Liu<sup>2</sup>, Bowen Guo<sup>1</sup>, Zeju Li<sup>1</sup>, Miao Zhao<sup>3</sup>, Wenhao Ju<sup>4</sup>, Zhiling Luo<sup>3</sup>,  
Xianhong Shu<sup>2\*</sup>, Yi Guo<sup>1\*</sup>, Yuanyuan Wang<sup>1\*</sup>

<sup>1</sup>Fudan University <sup>2</sup>Fudan Zhongshan Hospital <sup>3</sup>Fuwai Yunnan Hospital <sup>4</sup>Fuwai Beijing Hospital

## Abstract

*Reliable interpretation of echocardiography (Echo) is crucial for assessing cardiac function, which demands clinicians to synchronously orchestrate multiple capabilities, including visual observation (“eyes”), manual measurement (“hands”), and expert knowledge learning and reasoning (“minds”). While current task-specific deep-learning approaches and multimodal large language models have demonstrated promise in assisting Echo analysis through automated segmentation or reasoning, they remain focused on restricted skills, i.e., “eyes-hands” or “eyes-minds”, thereby limiting clinical reliability and utility. To address these issues, we propose EchoAgent, an agentic system tailored for end-to-end Echo interpretation, which achieves a fully coordinated “eyes-hands-minds” workflow that learns, observes, operates, and reasons like a cardiac sonographer. First, we introduce an expertise-driven cognition engine where our agent can automatically assimilate credible Echo guidelines into a structured knowledge base, thus constructing an Echo-customized “mind”. Second, we devise a hierarchical collaboration toolkit to endow EchoAgent with “eyes-hands”, which can automatically parse Echo video streams, identify cardiac views, perform anatomical segmentation, and quantitative measurement. Third, we integrate the perceived multimodal evidence with the exclusive knowledge base into an orchestrated reasoning hub to conduct explainable inferences. We evaluate EchoAgent on CAMUS and MIMIC-EchoQA datasets, which cover 48 distinct echocardiographic views spanning 14 cardiac anatomical regions. Experimental results show that EchoAgent achieves state-of-the-art performance across diverse cardiac structure function analyses, yielding overall accuracy scores of up to 80.00%. Importantly, EchoAgent empowers a single system with abilities to learn, observe, operate and reason like a cardiac sonographer, which holds great promise for delivering reliable and clinically-actionable Echo interpretation.*

## 1. Introduction

Echocardiography (Echo) stands as a widely used and indispensable non-invasive imaging modality for the assessment of cardiac function, forming the cornerstone of diagnosis, management, and prognostic evaluation across a broad spectrum of cardiovascular diseases [16, 27, 37]. The clinical value of Echo, however, is not fully uncovered through the simple observation of raw visual information [17, 34]. Instead, it is unlocked through expert interpretation as shown in Figure 1 (a), which is a complex, integrative task that requires clinicians to orchestrate multi-dimensional abilities, fundamentally encompassing (1) “eyes” for visual observation and view recognition across multiple cardiac views, (2) “hands” for precise structure localization and segmentation, as well as quantitative measurement of key parameters, and (3) “minds” for learning clinical knowledge, integrating multimodal evidence, and executing logical and reliable diagnostic reasoning.

The pursuit of automating Echo analysis has been a prevalent focus of medical Artificial Intelligence (AI) research [3, 10, 15, 18, 24, 28, 32, 39], primarily advancing along two types of paradigms, as displayed in Figure 1 (b). The first paradigm leverages task-specific deep learning (DL) models [10, 15, 18, 28], which excel in replicating the “eyes” and “hands” of clinicians, with excellent performance in isolated tasks such as view classification, anatomical structure segmentation, or parameter measurement. Nevertheless, these approaches fall short of performing full-study Echo interpretation as they lack the Echo “minds”, i.e., the ability to autonomously orchestrate distinct “hands” in a clinically-logical order and reason about the clinical significance of their operation results in Echo. Another type of paradigm employs Multimodal Large Language Models (MLLMs) [3, 24, 32, 39], which exhibit impressive abilities in visual question answering and semantic reasoning, offering a form of “eyes-minds” capability. MLLMs can describe image content and answer questions based on visual and textual patterns pretrained from vast datasets. Nonetheless, without specific knowl-

\*Corresponding authors

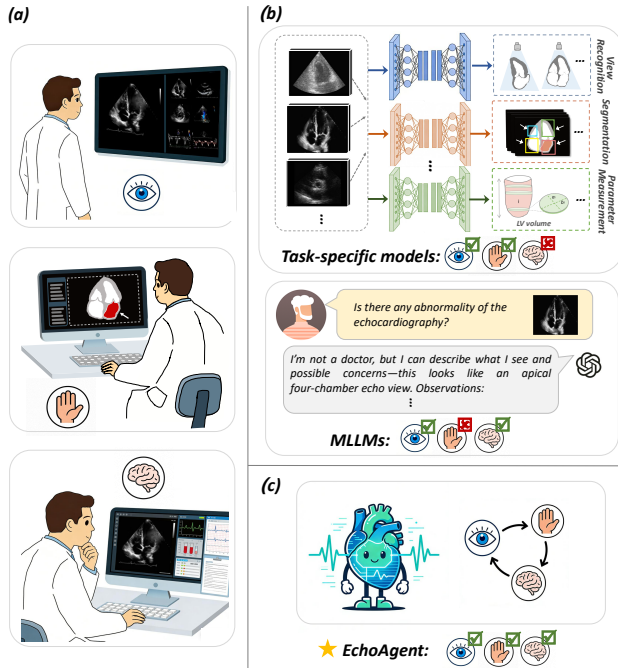


Figure 1. Motivations and challenges of Echo interpretation. Motivations: (a) Schematic diagram of clinical interpretation workflow. Challenges: (b) Current task-specific models lack cognitive faculties, while general MLLMs lack Echo-specific expertise and capabilities. (c) EchoAgent: An agentic system emulating expert interpretation with fully coordinated “eyes-hands-minds”.

edge ingrained for Echo and the precise “hands” for quantitative analysis, these models are hard to fulfill expert-level Echo interpretation as they lack domain-aware expertise and capabilities to obtain crucial quantitative evidence, i.e. Echo-specific “minds” and “hands”, which is often ungrounded and clinically unreliable [11, 30, 40]. Therefore, we still lack an end-to-end solution with integrated “eyes-hands-minds” for reliable Echo interpretation.

To tackle these issues, we propose EchoAgent, an agentic system specialized for end-to-end Echo interpretation. As illustrated in Figure 1 (c), we aim to design a workflow that emulates the perceptual-cognitive-motor process of a cardiac sonographer to learn, observe, operate, and reason. Specifically, EchoAgent accomplishes this through three stages. At the initial stage, our EchoAgent encompasses an essential domain-aware “mind” via a preliminary expertise-driven cognitive engine. Subsequently, it is operationalized through a hierarchical collaboration toolkit, empowered with “eyes” and “hands”. Ultimately, EchoAgent is capable of executing a fully coordinated “eyes-hands-minds” workflow under the orchestration of an orchestrated reasoning hub, thus performing reliable reasoning for cardiac function assessment. In short, our contributions can be summarized as follows:

- 1) We present a specialized agentic system for Echo interpretation, named EchoAgent, which not only performs re-

liable Echo analysis within a single framework, but also pioneers a novel “eyes-hands-minds” paradigm.

- 2) To endow EchoAgent with multi-dimensional capabilities, we design an expertise-driven cognition engine to build a foundational “mind” with domain-aware knowledge repository construction, followed by a hierarchical collaboration toolkit that functions as “eyes” and “hands” through diverse perception and operation skills.
- 3) Building upon the expertise knowledge base and integrated multimodal information, we further introduce an orchestrated reasoning hub that intelligently collaborates perception, operation, and reasoning abilities, thereby implementing stepwise and traceable Echo interpretation.
- 4) We conduct comprehensive evaluations of EchoAgent across 48 distinct views covering 14 key cardiac structures. Experimental results demonstrate that EchoAgent achieves state-of-the-art performance, exhibiting an analytical process that closely mimics the “eyes-hands-minds” coordination of human specialists.

## 2. Related work

### 2.1. Specialized task-specific networks for Echo

Developing DL networks to automate Echo analysis has become a trendy research objective [6, 10, 18, 26, 42]. Plenty of work has focused on specific sub-tasks, primarily including view identification and anatomical structure segmentation. Early approaches employed CNNs to identify views [21, 43], while recent advancements have utilized multi-instance learning[33] or pretrained foundation models (FMs) [9, 38] to capture complex visual patterns for accurate view prediction. For segmentation, U-Net remains the strong baseline [23], with attention mechanisms being adapted to improve boundary delineation for cardiac structures [15, 28, 31, 44]. Moving forward, the emergence of FMs have also spurred remarkable advances in Echo segmentation, where FM-based models such as MemSAM [10] and EchoONE [18] facilitate precise segmentation for Echo. While these models excel in their designated tasks, they operate with limited “eyes” and “hands”, requiring separate manual assistance for final diagnostic conclusion, which is not favorable for comprehensive Echo interpretation.

### 2.2. Advanced MLLMs in medicine

The advent of MLLMs has introduced a new paradigm for medical image understanding recently. Pre-trained on massive web-scale image-text pairs, pioneers like Qwen-VL [2, 4, 39], DeepSeek [14, 25, 41], and OpenAI-GPT [1, 19] series exhibit remarkable zero-shot or few-shot capabilities for image captioning and general visual question answering (VQA) in real-world scenarios. Various works have attempted to further pre-train or fine-tune models on biomedical corpora, yielding medical-specialized MLLMs such as

LLaVA-Med [24] and DeepSeek-R1-Distill-Llama-8B [19]. While they demonstrate impressive abilities to interpret and reason semantically, showcasing a basic form of “eyes-minds”, they remain fundamentally passive and discussion-oriented, given the absence of domain-specialized expertise and tool-oriented capabilities to acquire clinical evidence. Consequently, endowing MLLMs with expert “minds” and the dexterous “hands” for reliable Echo interpretation remains an urgent and necessary challenge.

### 2.3. Towards domain-expertise agentic system

Recent days have witnessed growing interest in developing autonomous agentic systems, driven by the unparalleled tool-calling capability of MLLMs most recently [3, 32]. This promotes the development of agents to transcend the conversational nature of standard MLLMs by actively orchestrating external tools to acquire quantitative evidence and execute complex workflows [7, 11, 30]. For instance, [11] introduces a pipeline MedRAX, integrating specialized CXR tools with MLLMs to address complex chest X-ray analysis. In the more generalized CT and X-ray domains, [30] enhances diagnostic performance by explicitly infusing MLLMs with knowledge from domain-specialized vision models. Meanwhile, [7] presents a collaborative-learning framework that adaptively incorporates pre-trained single-modal medical large models with small multimodal models to boost multimodal diagnosis. Despite these advances, we still lack a specialized agent for reliable Echo interpretation, since Echo is a unique imaging modality, characterized by its inherent multi-view interdependency, complex anatomical geometry, and ambiguous structure boundaries. These challenges necessitate a specialized synergy of Echo expertise with perceptual, operational, and reasoning capabilities, which existing agents are not designed to fulfill.

## 3. Method

### 3.1. Overview

Figure 2 depicts the overall framework of EchoAgent, which comprises three core stages. Mimicking consciousness cultivation of a cardiac sonographer, EchoAgent firstly formulates an essential Echo-specialized “mind” by adapting a general-purpose MLLM (i.e. Qwen3-VL-Plus [3]), which assimilates domain expertise in the form of clinical guidelines and medical literature through an expertise-driven cognition engine, converting heterogeneous textual information into a structured knowledge base. Afterwards, EchoAgent is equipped with requisite operating skills with a powerful combination of FMs within a hierarchical collaboration toolkit, implementing Echo video stream parsing, view identification, anatomical structure recognition and segmentation, as well as diverse quanti-

tative measurements. With “eyes”, “hands” and “minds”, EchoAgent finally can autonomously perform end-to-end Echo interpretation, with an orchestrated reasoning hub to receives the external clinical diagnostic query and raw Echo videos, which dynamically comprehends multimodal information, orchestrates the toolkit to gather patient-specific evidence, performs structured reasoning grounded to the knowledge repository, and finally draw an evidence-backed diagnostic conclusion.

### 3.2. Expertise-driven cognition engine

As one person needs to learn expertise knowledge to be a qualified echocardiographer, we devise an Expertise-Driven Cognition (EDC) engine to initialize a specialized “mind” of our agent, building a structured knowledge base for 48 cardiac views covering 14 structures of the heart.

To acquire textual knowledge for Echo, we mainly exploit four expertised sources, which consist of a medical library Unified Medical Language System (UMLS) [5] for general conception learning and specific Echo guidelines from the American Heart Association (AHA), American Society of Echocardiography (ASE) and European Association of Cardiovascular Imaging (EACVI) [13, 16, 27, 29, 34], which provide credible knowledge for view acquisition, anatomy regions, measurement techniques and diagnostic criteria. Furthermore, we transform heterogeneous domain knowledge into a machine-actionable repository through the dedicated EDC engine. First, documents from all sources are preprocessed and decomposed into semantically coherent knowledge primitive  $P = \{p_1, p_2, \dots, p_D\}$ . Each primitive is encoded by a medical concept encoder  $f_\theta(\cdot)$  and then mapped into a shared high-dimensional embedding space, thereby constructing a hierarchical topology over the knowledge corpus. This embedding process can be formulated as:

$$e_i = f_\theta(p_i), \quad (1)$$

where  $p_i$  denotes the  $i$ -th knowledge primitive and  $e_i$  represents its corresponding semantic representation.

To enable efficient and anatomy-aware knowledge access, we predefine 14 common cardiac anatomical groups  $A = \{a_1, a_2, \dots, a_{14}\}$ , including left ventricle, mitral valve, aortic valve and so forth. Each primitive  $p_i$  is assigned to one or more anatomical subsets, thus organized into anatomy-indexed subsets:

$$I_{a_j} = \{p_i \mid a_j \in A(p_i)\}, \quad (2)$$

Considering a target anatomy  $a_t$ , the agent first narrows the search to the corresponding subset  $I_{a_t}$  by performing anatomy-specific retrieval based on retrieval augmented generation (RAG) [12] to extract the  $k$  most relevant primitives. The relevance between the target keywords  $d_{a_t}$  and a

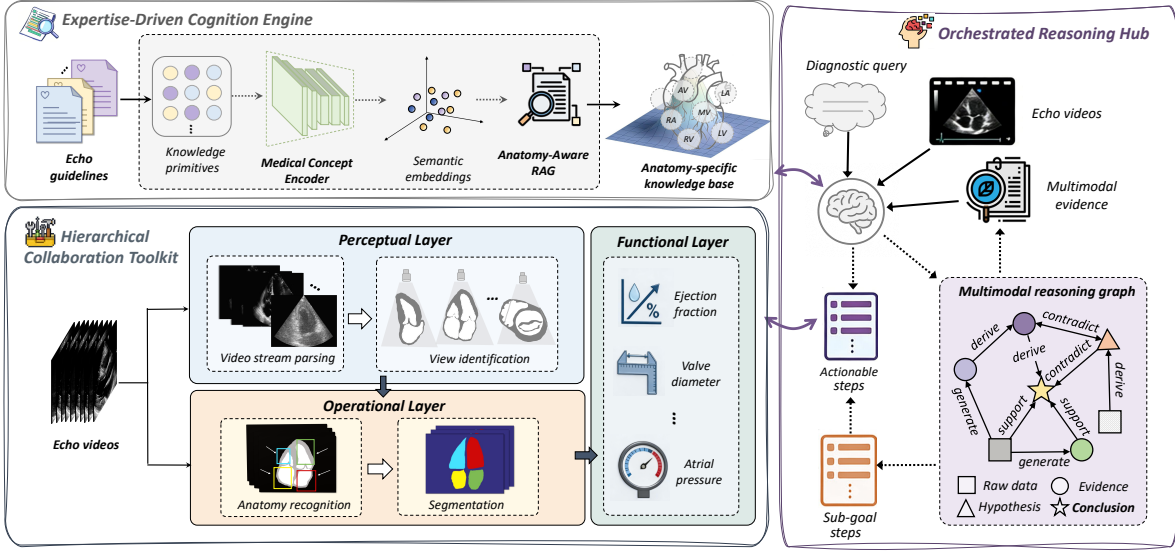


Figure 2. Framework of our EchoAgent, which establishes a fully coordinated workflow for Echo interpretation through an expertise-driven cognitive engine to build an essential Echo “mind”, a hierarchical collaboration toolkit that delivers manipulation skills, and an orchestrated reasoning hub to dynamically integrate these components, enabling evidence-based reasoning for cardiac function assessment.

primitive  $p_i$  measured by cosine similarity :

$$\text{sim}(w_{a_t}, p_i) = \frac{f_{\theta}(d_{a_t}) \cdot \mathbf{e}_i}{\|f_{\theta}(d_{a_t})\| \|\mathbf{e}_i\|}. \quad (3)$$

The top-k primitives with the highest similarity are retrieved:

$$P_{top-k} = \text{top}_k(\{\text{sim}(d_{a_t}, p_i) \mid p_i \in P_{a_t}\}). \quad (4)$$

Based on the retrieved primitives, we conduct structured summary and finally establish a machine-actionable knowledge repository  $\mathbf{R} = \{r_1, r_2, \dots, r_{a_t}, \dots\}$  for all essential cardiac anatomical structures.

### 3.3. Hierarchical collaboration toolkit

Upon the cultivation of a foundational Echo “mind”, we further introduce a Hierarchical Collaboration (HC) toolkit to endow EchoAgent with Echo-specific “eyes” and “hands”. The toolkit is assembled by three distinct layers, mirroring the progression from visual observation to manual operation and quantitative functional measurements.

**Perceptual layer:** We first design a perceptual layer to process the fundamental visual characteristics of Echo, which is inherently characterized by multi-view interdependency and complex spatiotemporal dynamics. To this end, we harness a dedicated FM, EchoPrime [38], to parse the input video streams and automatically identify the diverse echocardiographic views (e.g., apical-2-chamber, apical 4-chamber, parasternal long-axis) present within the sequence. The perceptual layer establishes the essential spatial and anatomical context for subsequent analysis.

**Operational layer:** Since the accurate segmentation of specific anatomical structures is a prerequisite for deriving clin-

ically meaningful quantitative metrics, we employ a customized segmentation model that has previously been devised based on USFM [20]. This layer performs the automatic delineation of key cardiac structures (e.g., left ventricle, aorta, right ventricle, left atrium), providing a robust foundation for the following functional analysis.

**Functional layer:** Building upon the outputs of the perceptual and operational layers, we further incorporate dedicated fine-tuned versions of USFM and EchoPrime to function as a specialized quantitative analysis engine, which is responsible for calculating critical clinical parameters, such as ejection fraction, chamber dimensions, and right atrial pressure, as well as generating clinical reports to assess function of distinct cardiac structures.

### 3.4. Orchestrated reasoning hub

Having possessed the specialized “eyes”, “hands”, and “mind”, we propose an Orchestrated Reasoning (OR) Hub to specially emulate the neurological system of a cardiac sonographer for reliable and end-to-end Echo interpretation, accomplishing a fully coordinated perception-action-reasoning workflow. Given a cardiac diagnostic query  $Q$  and the corresponding raw Echo videos  $V$ , the OR Hub initiates a closed-loop reasoning process tailored for Echo:

**1) Expertised Echo knowledge retrieval & task allocation:** The hub first interacts with the exclusive Echo knowledge repository  $\mathbf{R}$  stored in the foundational “mind”. According to Equation 3, it performs a latent semantic retrieval to find the the targeted repository  $\mathbf{R}_{a_q}$  relevant to  $Q$ :

$$\mathbf{R}_{a_q} = \arg \max_{r \in \mathbf{R}} \text{sim}(f_{\theta}(Q), e_i). \quad (5)$$

Subsequently, the hub decomposes  $\mathbf{r}_{a_q}$  into an actionable sequence of steps  $\mathbf{S} = \{s_1, s_2, \dots, s_n\}$ , where each step is

adaptively scheduled and mapped to the optimal functional tool in the HC toolkit  $\tau_{a_q}^* \in T$ . Thus, each step  $s_i$  can be defined as:

$$s_i : \text{Execute}(\tau_{a_q}^*, \text{Input}_i) \quad (6)$$

**2) Dynamic Echo reasoning graph construction:** As each step is executed, the HC Toolkit returns quantitative evidence based on Echo with confidence scores. Rather than forming premature conclusions, the OR Hub incrementally constructs a dynamic multimodal reasoning graph for Echo  $G = (N, E)$ , in which Nodes ( $N$ ) represent Echo-specific clinical entities: cardiac diagnostic concepts, execution evidence (with associated confidence scores), and raw data anchors. Edges ( $E$ ) represent Echo-specific clinical relationships, including:

- **Generation:** [Raw Data]–(generates)→[Evidence] (e.g., raw A2C video → LV segmentation mask).
- **Support/contradiction:** [EvidenceA] ← (supports /contradicts) → [Hypothesis/EvidenceB] (e.g., “EF=33.5%” ←→ “Considerably reduced EF/Normal”).
- **Derivation:** [Raw Data/EvidenceA]–(derives)→ [Hypothesis/EvidenceC] (e.g., LV segmentation mask → LV volume at different phrases → “EF=33.5%”).

**3) Adaptive Echo reasoning workflow:** To ensure robust Echo reasoning, the hub performs adaptive inferencing process. Specifically, it firstly considers confidence and evaluates the certainty between cardiac diagnostic hypotheses  $H = \{h_1, h_2, \dots\}$  and the current Echo evidence graph  $G(t)$ , where the posterior probability of each hypothesis is:

$$P(h_m|G(t)) \propto P(G(t)|h_m) \cdot P(h_m), \quad (7)$$

in which the likelihood  $P(h_m|G(t))$  is defined by evaluating the consistency of Echo-specific patterns under hypothesis  $h_m$  at time  $t$ .

If any step yields low confidence or high uncertainty, the hub triggers an adaptive Echo-focused mechanism to seek alternative diagnostic pathways, which will actively generate a set of sub-goal  $S_{sub}$  like requesting a re-measurement from a different view. The sub-goal will be inserted into the action step pool  $S$ . This iterative thinking process persists until the evidence graph achieves a sufficient consistency score or a maximum reasoning depth is reached, which ensures a verifiable and self-reflective reasoning trajectory.

Consequently, we have constructed a fully coordinated “eyes-hands-minds” workflow, realizing an end-to-end agentic system specifically engineered for Echo.

## 4. Experiments and analysis

### 4.1. Experiment setup

**Datasets:** We conduct experiments on two datasets CAMUS [23] and MIMIC-EchoQA [35], which present progressively challenging settings. The CAMUS dataset contains apical-2-chamber (A2C) and apical-4-chamber (A4C)

Table 1. Dataset statistics

Dataset		CAMUS (EF grading)			
Overall statistics	Subject number	Video number		Frame number	
	500	1000		9,268	
Specific cases	Normal (EF≥50%)	Mildly reduced (40%≤EF<50%)	Considerably reduced (EF<40%)		
	178	164	158		

Dataset		MIMIC-EchoQA (Multi-option question-answer)				
Overall statistics	Subject number	Video number		Frame number		
	622	622		51,194		
Specific cases	Pericardium	Aortic valve	Mitral valve	Ventricles	Atria	Vessels & Others
	82	132	87	190	73	58

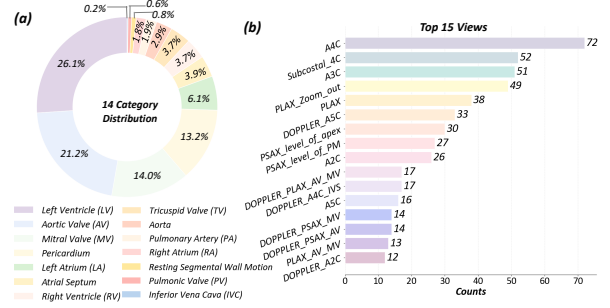


Figure 3. Detailed distribution of (a) cardiac structures and (b) top 15 views in the MIMIC-EchoQA dataset.

Echo videos with annotations for left ventricle (LV) and labels for ejection fraction (EF), which is essential to assess heart failure [16, 34]. The MIMIC-EchoQA benchmark is built from the MIMIC-IV-ECHO, encompassing 48 distinct views and covering 14 cardiac structures (grouped to 7 major categories), with multiple-choice clinical questions concerning assessment for structures such as pericardium, atria as well as ventricles, vessels and valves. The details of the datasets are summarized in Table 1 and Figure 3.

**Evaluation metrics:** For the EF grading task on the CAMUS dataset, we follow clinical guidelines [22, 34] to categorize cases into three grades. The overall classification performance is evaluated by the commonly used accuracy (Acc), and geometric mean (G-mean) to account for potential class imbalance. Moreover, we perform an area under the receiver operating characteristic curve (AUROC) analysis on EF to assess the quantification capability of those models with “hands”. For the MIMIC-EchoQA benchmark, where tasks are formulated as multiple-choice questions, we present the Acc indicator as detailed per-group Acc as well as the overall Acc across all questions.

**Implementation details:** We implement EchoAgent using PyTorch and LangChain [36] to orchestrate the agentic workflow. All experiments are conducted on a server equipped with an NVIDIA GeForce Tesla A100 GPU to ensure efficient finetuning of FMs and inference of MLLMs. For the base “mind”, we employ Qwen3-VL-Plus [3] as the backbone MLLM, which provides fundamental “eyes-

Table 2. Comparative results (Acc and G-mean, %) on the single-structure task (EF grading). ‘‘E’’, ‘‘H’’, and ‘‘M’’ represent ‘‘eyes’’, ‘‘hand’’ and ‘‘minds’’, respectively.  $\checkmark$  denotes the presence of the capability, while  $\times$  denotes absence, and  $\star$  denotes a specialized and coordinated state of presence. **Bold** numbers indicate the best performance.

Method	Capabilities			Normal		Mildly reduced		Considerably reduced		
	H	M	E-H-M	Acc	G-mean	Acc	G-mean	Acc	G-mean	
Task-specific models	OnimiaNet	$\checkmark$	$\times$	$\times$	74.00	64.81	74.00	71.76	78.00	83.62
	H2former	$\checkmark$	$\times$	$\times$	74.00	59.16	65.00	58.57	63.00	72.00
	MemSAM	$\checkmark$	$\times$	$\times$	73.00	52.29	53.00	46.06	60.00	69.44
	EchoONE	$\checkmark$	$\times$	$\times$	74.00	63.54	64.00	62.32	80.00	85.05
General-purpose models	LLaVA-Med	$\times$	$\checkmark$	$\times$	48.00	47.43	58.00	43.05	58.00	39.97
	Qwen2.5-7B-VL	$\times$	$\checkmark$	$\times$	39.00	12.58	58.00	0.00	79.00	0.00
	Deepseek-VL2	$\times$	$\checkmark$	$\times$	40.00	12.75	60.00	0.00	80.00	21.82
	GPT-5	$\times$	$\checkmark$	$\times$	44.00	44.72	61.00	0.00	55.00	52.08
‘‘E-H-M’’ workflows	GPT-5*	$\checkmark$	$\checkmark$	$\checkmark$	78.00	69.52	69.00	69.04	89.00	<b>92.78</b>
	<b>EchoAgent</b>	$\star$	$\star$	$\star$	<b>88.00</b>	<b>83.87</b>	<b>80.00</b>	<b>80.16</b>	<b>92.00</b>	89.60

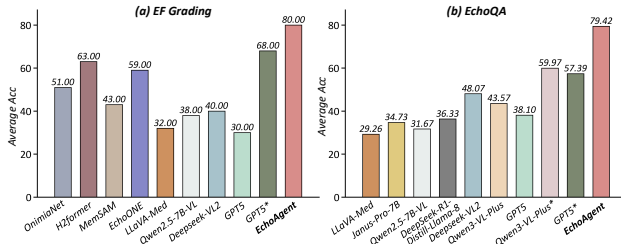


Figure 4. Average Acc in (a) EF grading and (b) EchoQA task.

‘‘minds’’ capabilities for processing general multimodal information and potential learning. In addition, we adhere to the official split ratio of 7:1:2 for training, validation, and testing in the CAMUS dataset, while treating all provided cases as held-out test cases for the MIMIC-EchoQA. Especially, EF in CAMUS is calculated based on segmentation results of LV according to Simpson’s biplane method of disks (SMOD) [22].

## 4.2. Comparison on the single-structure task

In order to validate the advantages of our method in the sophisticated task of Echo interpretation, we first conduct experiments on the single-structure (i.e., LV) task using the CAMUS dataset to evaluate fundamental cardiac function based on EF grading. Our comparison encompasses three types of paradigms:

- **Task-specific models:** Since LV segmentation is a prerequisite for accurate EF calculation, we evaluate four approaches specifically designed for Echo segmentation, including two customized networks H2former [15] and OnimiaNet [28], along with two fine-tuned FMs MemSAM [10] and EchoONE [18].
- **General-purpose models:** To assess the capability of current MLLMs for Echo reasoning, we benchmark against four representative models, i.e., LLaVA-Med [24], Qwen2.5-7B-VL [39], DeepSeek-VL2 [41], as well as the latest GPT-5 [32].
- **‘‘E-H-M’’ workflows:** For a more equitable comparison that isolates the benefit of coordination, we adapt the lat-

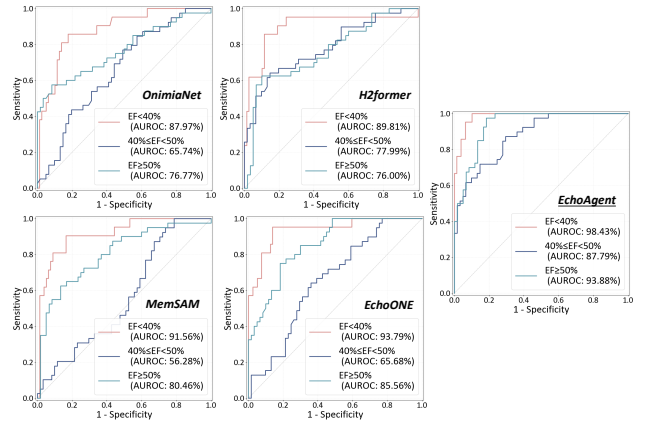


Figure 5. ROC curves for LVEF in the CAMUS dataset, derived from segmentation results of models with ‘‘hands’’.

est baseline GPT-5 which possesses the latent tool-calling capability, into an enhanced GPT-5\*, The enhanced configuration equips GPT-5 with the same ‘‘hands’’ (i.e., HC toolkit) used in our proposed pipeline, thus further testing whether simply augmenting a powerful MLLM with tools is sufficient for Echo analysis.

Table 2 and Figure 4 (a) present the quantitative comparison among 10 approaches.

In particular, task-specific models [10, 15, 18, 28] deliver competitive performance with Acc and G-mean exceeding 63.00% and 58.00%, respectively, which can be attributed to their specialized capability to operate as skilled ‘‘hands’’ for segmentation. However, these models need extra assistance to complete the full diagnostic grading workflow. Instead, general-purpose MLLMs [24, 32, 39, 41] can execute the task autonomously, yet their performance lags behind task-specific counterparts, with a maximum accuracy drop of 30.00% and notably low G-mean scores. This may be due to their lack of fine-grained perceptual ‘‘hands’’, which are critical for complicated Echo interpretation. This highlights the inherent difficulty of precisely interpreting Echo using models with only limited or isolated capabilities.

Hence, we enhance GPT-5 into GPT-5\*, which possesses

Table 3. Comparative performance (Acc, %) of the EchoAgent with state-of-the-art MLLMs on the multi-structure task (EchoQA).

Method	Pericardium	Aortic valve	Mitral valve	Ventricles	Atria	Vessels	Others
LLaVA-Med	32.93	20.45	20.69	30.53	35.62	41.94	48.15
Janus-Pro-7B	39.02	26.52	27.59	40.53	30.14	51.61	37.04
Qwen2.5-7B-VL	50.00	18.18	29.89	36.84	27.40	25.81	29.63
DeepSeek-R1-Distill-Llama-8B	41.46	30.30	27.59	38.42	41.10	45.16	40.74
Deepseek-VL2	74.39	51.52	52.87	32.63	52.05	41.94	40.74
Qwen3-VL-Plus	65.85	43.18	43.68	36.32	53.42	35.48	11.11
GPT-5	60.98	40.91	36.78	26.32	36.99	38.71	44.44
Qwen3-VL-Plus*	73.17	56.82	56.32	57.37	69.86	48.39	51.85
GPT-5*	69.51	60.61	59.77	47.89	63.01	41.94	66.67
<b>EchoAgent</b>	<b>84.15</b>	<b>82.58</b>	<b>81.61</b>	<b>75.26</b>	<b>80.82</b>	<b>77.42</b>	<b>70.37</b>

a basic coordinated workflow. GPT-5\* yields a notable improvement over the standard GPT-5, increasing the average Acc from 30.00% to 68.00%. This confirms that augmenting general-purpose “mind” with specialized Echo “hands” is not only beneficial but essential for Echo interpretation. However, its performance remained inferior, particularly in the “Mildly reduced” grade with both Acc and G-mean less than 69.10%, indicating that the mere tool access is insufficient for generalized Echo diagnosis. In contrast, the proposed EchoAgent achieves superior performance, surpassing all competitors with an average Acc of 80.00%. Specifically, EchoAgent attains the highest Acc of 88.0%, 80.0%, and 92.0%, as well as G-mean of 83.87% , 80.16% , and 89.60% across three grades.

To further assess the operational utility, we conducted a ROC analysis on LVEF at clinical thresholds among those models with “hands”, as shown in Figure 5. EchoAgent yields remarkable AUROC scores of 98.43%, 87.79%, and 93.88% for three EF grading thresholds, respectively. These consistently discriminative performances indicate the robust ability to reliably identify patients with systolic dysfunction requiring prompt intervention, while minimizing unnecessary follow-up examinations. Collectively, these results demonstrate that EchoAgent accomplishes superior performance in LV function assessment, verifying the effectiveness of the “eyes-hands-minds” coordination.

### 4.3. Comparison on the multi-structure task

To further evaluate the diagnostic breadth and reasoning capability, we carry out experiments on the multi-structure task in the MIMIC-EchoQA dataset, which assesses cardiac function across 7 major anatomical groups with raw Echo videos and clinical question-option pairs. Table 3 and Figure 4 (b) present the comparative results of EchoAgent with various MLLMs.

It is evident that EchoAgent demonstrates balanced and generalized proficiency across all anatomical categories, whereas the representative MLLMs exhibit inconsistent and limited performance. In concrete, pioneers such as LLaVA-Med [24], Janus-Pro-7B [8], Qwen2.5-7B-VL [39] and DeepSeek-R1-Distill-Llama-8B [14] provide a baseline level of results and performs relatively well on cer-

tain anatomy, obtaining best scores of 48.15% for “Others”, 51.61% for “Vessels”, 50.00% for “Pericardium” and 45.16% for “Vessels”, respectively. They all struggle on other structures, where corresponding Acc can be as low as 20.45%, 26.52%, 18.18%, and 30.30% for the clinically-significant cardiac valve “Aortic valve”. Especially, Deepseek-VL2 [41] excels at pericardium, reaching a score up to 74.39%. However, its accuracy on the remaining six structural groups remains around 40%, showcasing an inability to generalize across diverse cardiac anatomy. Moreover, the most recent MLLMs Qwen3-VL-Plus [3] and GPT-5 [32] show moderate improvements in certain categories, yet they still exhibit severe performance limitations. Particularly, GPT-5 achieves only 26.32% on “Ventricles”, and Qwen3-VL-Plus drops to 11.11% on the “Others” category. Nonetheless, when updated to Qwen3-VL-Plus\* and GPT-5\*, their performances show consistent increases of 16.40% and 19.29%. This indicates that specialized tools are indispensable for competent Echo interpretation.

However, even in their enhanced forms, Qwen3-VL-Plus\* and GPT-5\* exhibit notable disadvantages in minor categories, e.g., achieving Acc of only 48.39% and 41.94% in “Vessels”. In comparison, EchoAgent delivers consistently advantageous and balanced performance, with Acc scores above 70.37% for every anatomical structure. Notably, EchoAgent excels on challenging yet clinically pivotal structures such as the “Ventricles”, improving Acc by at least 34.73% over all compared MLLMs. On average, it surpasses the optimal MLLM and latest GPT-5 by 31.45% and 49.36%, respectively. This superior and stable performance can be attributed to the integrated “eyes-hands-minds” workflow of EchoAgent, which actively coordinates perception, measurement, and reasoning rather than relying on heuristics or biased attentions.

In addition, to further validate the merits of the integrated “eyes-hands-minds” workflow, we exemplify the inference processes of our EchoAgent with the lately published GPT-5 and Qwen3-VL-Plus in Figure 6. It can be observed that while general-purpose MLLMs can produce basic thoughts and coherent textual responses for Echo diagnostic questions, their reasoning processes still lack explicit guidance from clinical knowledge and fall short of a traceable chain

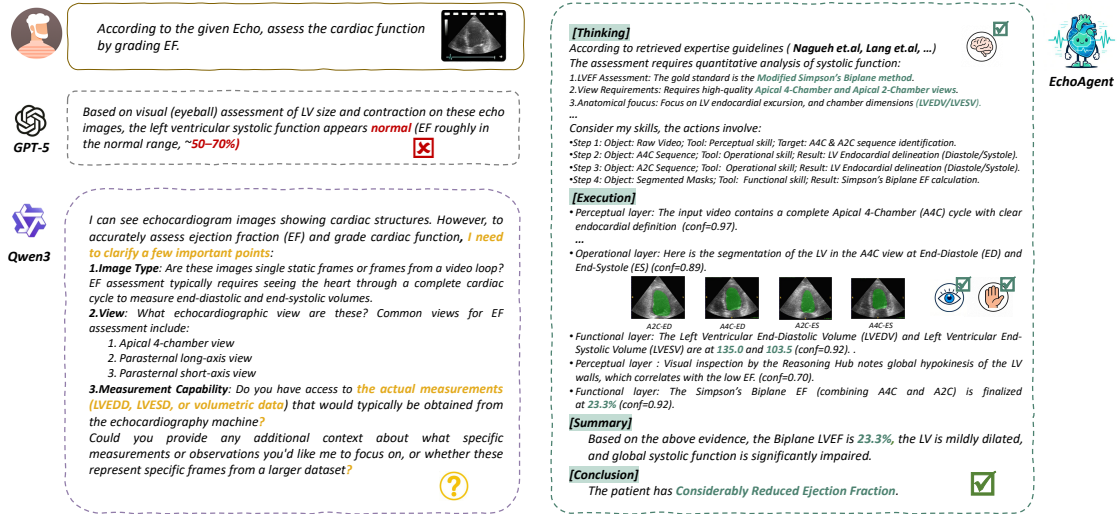


Figure 6. A case study for diagnostic analysis of our proposed EchoAgent, compared with two latest MLLMs [3, 32].

of evidence. Conversely, EchoAgent provides a structured, evidence-based, and grounded reasoning pathway, which is more favorable in clinical practice.

#### 4.4. Ablation studies

To rigorously evaluate the contribution of three core capabilities, we conduct ablation studies for both tasks. Our experiments begin with a reasoning baseline implemented on Qwen3-VL-Plus, which possesses the fundamental ability to process general multimodal information. We then sequentially investigate the importance of specialized components by: 1) adding the EDC engine to study the effect of a domain-specialized “mind”, 2) the HC toolkit to assess the contribution of skilled “hands”, and 3) integrating both the EDC engine and the HC toolkit under the coordination of the OR hub to construct the complete EchoAgent agent. The overall accuracy is reported in Table 4.

**The necessity of a specialized “mind”:** The baseline delivers limited Acc scores of less than 45%. By instilling a specialized “mind” through the EDC engine, the model exhibits marked performance improvements, with an increase of 15.00% for EF grading and 7.88% for the EchoQA task. These results confirm that a domain-aware reasoning foundation is essential for moving beyond generic visual understanding toward Echo-specific interpretation.

**The power of skilled “hands”:** Similarly, equipping the system with the HC toolkit also brings enhancement. Compared to the baseline, the HC toolkit raises mean Acc by 37.00% and 16.40% for the two tasks separately. In particular, the rise in EF Grading is notable, which may be owing to the fact that EF calculation is inherently dependent on skilled operation ability to perform accurate anatomy segmentation in clinical. These results underscore the significance of fine-grained operational skills, as reliable cardiac analysis necessitates quantitative evidence.

Table 4. Effectiveness (average Acc,%) of three core components.

Configuration	E	H	M	EF Grading	EchoQA
Baseline	✓	✗	✓	35.00	43.57
Baseline+EDC	✓	✗	★	50.00	51.45
Baseline+HC	✓	✓	✗	73.00	59.97
<b>Baseline+EDC+HC+OR</b>	<b>★</b>	<b>★</b>	<b>★</b>	<b>80.00</b>	<b>79.42</b>

**The synergy of integrated “eyes-hands-minds”:** When the EDC engine (specialized “mind”) and the HC toolkit (skilled “hands”) are incorporated and dynamically coordinated by the OR hub, EchoAgent accomplishes the optimal performance, reaching overall accuracy of up to 80.00%. It significantly outperforms configurations that possess only the EDC engine or only the HC toolkit, with maximal improvements of 45.00% and 35.85% for the EF grading task and knowledge-intensive EchoQA task, respectively. These demonstrate that the orchestrated synergy of “eyes-hands-minds” plays an indispensable role in the reliable end-to-end Echo interpretation.

## 5. Conclusion

In this paper, we propose EchoAgent, an agentic system to emulate the perceptual-cognitive-motor process of a cardiac sonographer to learn, observe, operate, and reason, which establishes a reliable and traceable way from raw Echo data to comprehensive Echo interpretation. To achieve this, we introduce an expertise-driven cognitive engine, a hierarchical collaboration toolkit, and an orchestrated reasoning hub to equip the agent with “eyes-hands-minds”. EchoAgent highlights the need to think how to adapt the “eyes-hands-minds” coordination process of humans to an agent for automated and reliable Echo interpretation. We believe EchoAgent can serve as a practical, trustworthy, and powerful assistant to enhance the clinical workflow of Echo diagnosis.



## Acknowledgements

This work was supported by National Natural Science Foundation of China (Grant NO. 62531004) and National Key R&D Program of China (2024YFF0507303).

## References

- [1] Josh Achiam, Steven Adler, Sandhini Agarwal, Lama Ahmad, Ilge Akkaya, Florencia Leoni Aleman, Diogo Almeida, Janko Altschmidt, Sam Altman, Shyamal Anadkat, et al. Gpt-4 technical report. *arXiv preprint arXiv:2303.08774*, 2023. 2
- [2] Jinze Bai, Shuai Bai, Yunfei Chu, Zeyu Cui, Kai Dang, Xiaodong Deng, Yang Fan, Wenbin Ge, Yu Han, Fei Huang, et al. Qwen technical report. *arXiv preprint arXiv:2309.16609*, 2023. 2
- [3] Shuai Bai, Yuxuan Cai, Ruizhe Chen, Keqin Chen, Xionghui Chen, Zesen Cheng, Lianghao Deng, Wei Ding, Chang Gao, Chunjiang Ge, et al. Qwen3-vl technical report. *arXiv preprint arXiv:2511.21631*, 2025. 1, 3, 5, 7, 8
- [4] Shuai Bai, Keqin Chen, Xuejing Liu, Jialin Wang, Wenbin Ge, Sibao Song, Kai Dang, Peng Wang, Shijie Wang, Jun Tang, et al. Qwen2.5-vl technical report. corr. abs/2502.13923, 2025. doi: 10.48550. *arXiv preprint ARXIV.2502.13923*, 2025. 2
- [5] Olivier Bodenreider. The unified medical language system (umls): integrating biomedical terminology. *Nucleic acids research*, 32(suppl\_1):D267–D270, 2004. 3
- [6] Chieh-Ju Chao, Yunqi Richard Gu, Wasan Kumar, Tiange Xiang, Lalith Appari, Justin Wu, Juan M Farina, Rachael Wraith, Jiwoon Jeong, Reza Arsanjani, et al. Foundation versus domain-specific models for left ventricular segmentation on cardiac ultrasound. *npj Digital Medicine*, 8(1):341, 2025. 2
- [7] Wanyi Chen, Zihua Zhao, Jiangchao Yao, Ya Zhang, Jiajun Bu, and Haishuai Wang. Multi-modal medical diagnosis via large-small model collaboration. In *Proceedings of the Computer Vision and Pattern Recognition Conference*, pages 30763–30773, 2025. 3
- [8] Xiaokang Chen, Zhiyu Wu, Xingchao Liu, Zizheng Pan, Wen Liu, Zhenda Xie, Xingkai Yu, and Chong Ruan. Janus-pro: Unified multimodal understanding and generation with data and model scaling. *arXiv preprint arXiv:2501.17811*, 2025. 7
- [9] Matthew Christensen, Milos Vukadinovic, Neal Yuan, and David Ouyang. Vision–language foundation model for echocardiogram interpretation. *Nature Medicine*, 30(5): 1481–1488, 2024. 2
- [10] Xiaolong Deng, Huisi Wu, Runhao Zeng, and Jing Qin. Memsam: Taming segment anything model for echocardiography video segmentation. In *Proceedings of the IEEE/CVF Conference on Computer Vision and Pattern Recognition*, pages 9622–9631, 2024. 1, 2, 6
- [11] Adibvafa Fallahpour, Jun Ma, Alif Munim, Hongwei Lyu, and Bo Wang. Medrax: Medical reasoning agent for chest x-ray. *arXiv preprint arXiv:2502.02673*, 2025. 2, 3
- [12] Yunfan Gao, Yun Xiong, Xinyu Gao, Kangxiang Jia, Jinliu Pan, Yuxi Bi, Yixin Dai, Jiawei Sun, Haofen Wang, Haofen Wang, et al. Retrieval-augmented generation for large language models: A survey. *arXiv preprint arXiv:2312.10997*, 2(1):32, 2023. 3
- [13] Julia Grapsa, Edgar Argulian, and Otto A Smiseth. Diastolic dysfunction: a comparison of 2025 ase, 2024 bse and 2022 eacvi guidelines, 2025. 3
- [14] Daya Guo, Dejian Yang, Haowei Zhang, Junxiao Song, Peiyi Wang, Qihao Zhu, Runxin Xu, Ruoyu Zhang, Shirong Ma, Xiao Bi, et al. Deepseek-r1: Incentivizing reasoning capability in llms via reinforcement learning. *arXiv preprint arXiv:2501.12948*, 2025. 2, 7
- [15] Along He, Kai Wang, Tao Li, Chengkun Du, Shuang Xia, and Huazhu Fu. H2former: An efficient hierarchical hybrid transformer for medical image segmentation. *IEEE Transactions on Medical Imaging*, 42(9):2763–2775, 2023. 1, 2, 6
- [16] Paul A Heidenreich, Biykem Bozkurt, David Aguilar, Larry A Allen, Joni J Byun, Monica M Colvin, Anita Deswal, Mark H Drazner, Shannon M Dunlay, Linda R Evers, et al. 2022 aha/acc/hfsa guideline for the management of heart failure: executive summary: a report of the american college of cardiology/american heart association joint committee on clinical practice guidelines. *Journal of the American College of Cardiology*, 79(17):1757–1780, 2022. 1, 3, 5
- [17] Gregory Holste, Evangelos K Oikonomou, Márton Tokodi, Attila Kovács, Zhangyang Wang, and Rohan Khera. Complete ai-enabled echocardiography interpretation with multi-task deep learning. *JAMA*, 334(4):306–318, 2025. 1
- [18] Jiongtong Hu, Wufeng Xue, Jun Cheng, Yingying Liu, Wei Zhuo, and Dong Ni. Echoone: segmenting multiple echocardiography planes in one model. In *Proceedings of the computer vision and pattern recognition conference*, pages 5207–5216, 2025. 1, 2, 6
- [19] Aaron Hurst, Adam Lerer, Adam P Goucher, Adam Perelman, Aditya Ramesh, Aidan Clark, AJ Ostrow, Akila Welihinda, Alan Hayes, Alec Radford, et al. Gpt-4o system card. *arXiv preprint arXiv:2410.21276*, 2024. 2, 3
- [20] Jing Jiao, Jin Zhou, Xiaokang Li, Menghua Xia, Yi Huang, Lihong Huang, Na Wang, Xiaofan Zhang, Shichong Zhou, Yuanyuan Wang, et al. Usfm: A universal ultrasound foundation model generalized to tasks and organs towards label efficient image analysis. *Medical image analysis*, 96:103202, 2024. 4
- [21] Hanan Khamis, Grigoriy Zurakhov, Vered Azar, Adi Raz, Zvi Friedman, and Dan Adam. Automatic apical view classification of echocardiograms using a discriminative learning dictionary. *Medical image analysis*, 36:15–21, 2017. 2
- [22] Roberto M Lang, Luigi P Badano, Victor Mor-Avi, Jonathan Afilalo, Anderson Armstrong, Laura Ernande, Frank A Flachskampf, Elyse Foster, Steven A Goldstein, Tatiana Kuznetsova, et al. Recommendations for cardiac chamber quantification by echocardiography in adults: an update from the american society of echocardiography and the european association of cardiovascular imaging. *European Heart Journal-Cardiovascular Imaging*, 16(3):233–271, 2015. 5, 6

- [23] Sarah Leclerc, Erik Smistad, Joao Pedrosa, Andreas Østvik, Frederic Cervenansky, Florian Espinosa, Torvald Espeland, Erik Andreas Rye Berg, Pierre-Marc Jodoin, Thomas Grenier, et al. Deep learning for segmentation using an open large-scale dataset in 2d echocardiography. *IEEE transactions on medical imaging*, 38(9):2198–2210, 2019. 2, 5
- [24] Chunyuan Li, Cliff Wong, Sheng Zhang, Naoto Usuyama, Haotian Liu, Jianwei Yang, Tristan Naumann, Hoifung Poon, and Jianfeng Gao. Llava-med: Training a large language-and-vision assistant for biomedicine in one day. *Advances in Neural Information Processing Systems*, 36:28541–28564, 2023. 1, 3, 6, 7
- [25] Aixin Liu, Bei Feng, Bing Xue, Bingxuan Wang, Bochao Wu, Chengda Lu, Chenggang Zhao, Chengqi Deng, Chenyu Zhang, Chong Ruan, et al. Deepseek-v3 technical report. *arXiv preprint arXiv:2412.19437*, 2024. 2
- [26] Jie Liu, Tiexin Qin, Hui Liu, Yilei Shi, Lichao Mou, Xiao Xiang Zhu, Shiqi Wang, and Haoliang Li. Q-part: quasi-periodic adaptive regression with test-time training for pediatric left ventricular ejection fraction regression. In *Proceedings of the Computer Vision and Pattern Recognition Conference*, pages 15560–15569, 2025. 2
- [27] Writing Committee Members, Catherine M Otto, Rick A Nishimura, Robert O Bonow, Blase A Carabello, John P Erwin III, Federico Gentile, Hani Jneid, Eric V Krieger, Michael Mack, et al. 2020 acc/aha guideline for the management of patients with valvular heart disease: a report of the american college of cardiology/american heart association joint committee on clinical practice guidelines. *Journal of the American College of Cardiology*, 77(4):e25–e197, 2021. 1, 3
- [28] Hicham Messaoudi, Ahror Belaid, Douraied Ben Salem, and Pierre-Henri Conze. Cross-dimensional transfer learning in medical image segmentation with deep learning. *Medical image analysis*, 88:102868, 2023. 1, 2, 6
- [29] Sherif F Nagueh, Danita Y Sanborn, Jae K Oh, Bonita Anderson, Kristen Billick, Genevieve Derumeaux, Allan Klein, Konstantinos Koulgiannis, Carol Mitchell, Amil Shah, et al. Recommendations for the evaluation of left ventricular diastolic function by echocardiography and for heart failure with preserved ejection fraction diagnosis: an update from the american society of echocardiography. *Journal of the American Society of Echocardiography*, 38(7):537–569, 2025. 3
- [30] Vishwesh Nath, Wenqi Li, Dong Yang, Andriy Myronenko, Mingxin Zheng, Yao Lu, Zhijian Liu, Hongxu Yin, Yee Man Law, Yucheng Tang, et al. Vila-m3: Enhancing vision-language models with medical expert knowledge. In *Proceedings of the Computer Vision and Pattern Recognition Conference*, pages 14788–14798, 2025. 2, 3
- [31] Nathan Painchaud, Nicolas Duchateau, Olivier Bernard, and Pierre-Marc Jodoin. Echocardiography segmentation with enforced temporal consistency. *IEEE transactions on medical imaging*, 41(10):2867–2878, 2022. 2
- [32] Aaditya Singh, Adam Fry, Adam Perelman, Adam Tart, Adi Ganesh, Ahmed El-Kishky, Aidan McLaughlin, Aiden Low, AJ Ostrow, Akhila Ananthram, et al. Openai gpt-5 system card. *arXiv preprint arXiv:2601.03267*, 2025. 1, 3, 6, 7, 8
- [33] Shanshan Song, Yi Qin, Honglong Yang, Taoran Huang, Hongwen Fei, and Xiaomeng Li. Echoviewclip: Advancing video quality control through high-performance view recognition of echocardiography. In *International Conference on Medical Image Computing and Computer-Assisted Intervention*, pages 181–191. Springer, 2025. 2
- [34] Cynthia C Taub, Raymond F Stainback, Theodore Abraham, Daniel Forsha, Enrique Garcia-Sayan, Jeffrey C Hill, Judy Hung, Carol Mitchell, Vera H Rigolin, Vandana Sachdev, et al. Guidelines for the standardization of adult echocardiography reporting: recommendations from the american society of echocardiography. *Journal of the American Society of Echocardiography*, 38(9):735–774, 2025. 1, 3, 5
- [35] Rahul Thapa, Andrew Li, Qingyang Wu, Bryan He, Yuki Sahashi, Christina Binder-Rodriguez, Angela Zhang, David Ouyang, and James Zou. Mimic-iv-echo-ext-mimicechoqa: A benchmark dataset for echocardiogram-based visual question answering. *PhysioNet*. 5
- [36] Oguzhan Topsakal and Tahir Cetin Akinci. Creating large language model applications utilizing langchain: A primer on developing llm apps fast. In *International conference on applied engineering and natural sciences*, pages 1050–1056, 2023. 5
- [37] AS Update. Heart disease and stroke statistics–2017 update. *Circulation*, 135(e146-e603):1, 2017. 1
- [38] Milos Vukadinovic, I-Min Chiu, Xiu Tang, Neal Yuan, Tien-Yu Chen, Paul Cheng, Debiao Li, Susan Cheng, Bryan He, and David Ouyang. Comprehensive echocardiogram evaluation with view primed vision language ai. *Nature*, pages 1–3, 2025. 2, 4
- [39] Peng Wang, Shuai Bai, Sinan Tan, Shijie Wang, Zhihao Fan, Jinze Bai, Keqin Chen, Xuejing Liu, Jialin Wang, Wenbin Ge, et al. Qwen2-vl: Enhancing vision-language model’s perception of the world at any resolution. *arXiv preprint arXiv:2409.12191*, 2024. 1, 2, 6, 7
- [40] Ziyue Wang, Junde Wu, Linghan Cai, Chang Han Low, Xihong Yang, Qiakuan Li, and Yueming Jin. Medagentpro: Towards evidence-based multi-modal medical diagnosis via reasoning agentic workflow. *arXiv preprint arXiv:2503.18968*, 2025. 2
- [41] Zhiyu Wu, Xiaokang Chen, Zizheng Pan, Xingchao Liu, Wen Liu, Damai Dai, Huazuo Gao, Yiyang Ma, Chengyue Wu, Bingxuan Wang, et al. Deepseek-vl2: Mixture-of-experts vision-language models for advanced multimodal understanding. *arXiv preprint arXiv:2412.10302*, 2024. 2, 6, 7
- [42] Jiewen Yang, Yiqun Lin, Bin Pu, Jiarong Guo, Xiaowei Xu, and Xiaomeng Li. Cardiacnet: Learning to reconstruct abnormalities for cardiac disease assessment from echocardiogram videos. In *European Conference on Computer Vision*, pages 293–311. Springer, 2024. 2
- [43] Jeffrey Zhang, Sravani Gajjala, Pulkit Agrawal, Geoffrey H Tison, Laura A Hallock, Lauren Beussink-Nelson, Mats H Lassen, Eugene Fan, Mandar A Aras, ChaRandle Jordan, et al. Fully automated echocardiogram interpretation in clinical practice: feasibility and diagnostic accuracy. *Circulation*, 138(16):1623–1635, 2018. 2

- [44] Zhenxuan Zhang, Heye Zhang, Tiejong Zeng, Guang Yang, Zhenquan Shi, and Zhifan Gao. Bridging multi-level gaps: Bidirectional reciprocal cycle framework for text-guided label-efficient segmentation in echocardiography. *Medical Image Analysis*, 102:103536, 2025. [2](#)